Journal of Human Ecology and Sustainability

Citation
Rubin, A. K. B., Austero, S. B., Orozco, C. R., & Resurrecion, A. C. (2024). Determination of the Effect of Manganese(II) on the Removal of Arsenic in Contaminated Water (Spiked Solution) using Electrochemical Arsenic Remediation (ECAR). *Journal of Human Ecology and Sustainability, 2*(3), 4.
doi: 10.56237/jhes24ichspd06

Corresponding Author
Austin Kinn B. Rubin
Email
abrubin@alum.up.edu.ph

Academic Editor
Casper B. Agaton

Received: 31 July 2024
Revised: 19 November 2024
Accepted: 24 November 2024
Published: 28 November 2024

Funding Information
This study is under the Philippine Electrochemical Arsenic Remediation (PHIL-ECAR-I) Project funded by CHED-PCARI and implemented by the University of the Philippines Diliman.

Original Research Article

Determination of the Effect of Manganese(II) on the Removal of Arsenic in Contaminated Water (Spiked Solution) using Electrochemical Arsenic Remediation (ECAR)

Austin Kinn B. Rubin [1], Sheila B. Austero [2], Christian R. Orozco [1], and Augustus C. Resurreccion [1]

[1] *Institute of Civil Engineering, University of the Philippines Diliman, Quezon City, 1101, Philippines*
[2] *Department of Community and Environmental Resource Planning, College of Human Ecology, University of the Philippines Los Baños, College 4031, Laguna, Philippines*

Abstract

Sustainable Development Goals (SDGs) 3, 6, and 11 emphasize the need for safe and clean water to create livable and sustainable human settlements. Arsenic contamination poses a significant challenge to these goals, threatening water safety and community health. Electrochemical Arsenic Remediation (ECAR) is an effective method for arsenic removal in water but is dependent on factors such as pH, dissolved oxygen, and ions such as calcium and magnesium. Electrocoagulation experiments were performed to determine the effect of manganese on the arsenic removal of ECAR at a low charge loading rate (5C/L) using arsenic and arsenic-manganese solutions. Results show that the percent arsenic removal for the control setup ranges from 61-96% and approximately 100% for the arsenic-manganese setup. The presence of 500 ppb manganese in the solution reduced arsenic concentration below the 10 ppb maximum limit set by WHO and DOH for drinking water for all arsenic-manganese setup which indicates that manganese has the potential to aid arsenic removal in water even at a low charge loading rate. Complete removal of manganese from the solution after ECAR was also observed. Statistical analysis shows that manganese and initial arsenic concentration significantly affect arsenic removal with an average estimated marginal effect of 0.4078 and 1.778, respectively. Results consequently illustrate that ECAR is a viable and effective technology in helping achieve SDGs 3, 6, and 11.

Keywords— arsenic, electrochemical, manganese, groundwater, remediation

1 Introduction

Access to safe and clean water is a fundamental human right and a pillar of sustainable development. The United Nations has emphasized this through Sustainable Development Goal (SDG) 6, which aims to "ensure availability and sustainable management of water and sanitation for all" and SDG 3 Target 3.9, which aims to "substantially reduce the number of deaths and illness from hazardous chemicals and air, water and soil pollution and contamination" by 2030 [1]. This goal is directly linked to SDG 11, which seeks to "make cities and human settlements inclusive, safe, resilient and sustainable" [1]. The link between these goals highlights the critical role of access to safe and clean water in creating livable and sustainable human settlements.

Without reliable access to safe and clean water, communities and settlements face significant health risks, economic challenges, and barriers to social development [2]. As global urbanization increases rapidly, the pressure on water resources and infrastructure in human settlements continues to rise [3]. To adapt to the growing demand for water resources, groundwater is increasingly preferred over surface water as the source of drinking water due to its availability, practicality, and affordability [4]. Natural groundwater contains cations and anions. According to the study conducted by Husana & Yamamuro [5], the primary ions found in Philippine groundwater are calcium(II), magnesium(II), sodium, potassium, ammonium ion, chloride, nitrite and nitrate, bromide, and sulfate. However, groundwater contamination of heavy metals such as arsenic presents a significant obstacle in achieving SDG 3, SDG 6 and SDG 11 since it threatens the safety of groundwater supply and, thus, the overall health of human settlements and communities.

In 2020, Solis et al. [6] found that the groundwater samples in the municipality of Guagua in the province of Pampanga were found to contain arsenic(As) concentrations as high as 95 parts per billion (ppb), which is above the 10 ppb limit set by the World Health Organization (WHO) [7] and by the Department of Health (DOH) [8] under the Philippine National Standards for Drinking Water of 2017. Similarly, Apostol et al. [9] also reported groundwater contamination of arsenic in the province of Batangas. They found out that 12 out of 14 (85.71%) wells used as a source of drinking water found in the municipalities surrounding the Taal Volcano in 2020 and 2021 have arsenic concentrations between 10 ppb to 39 ppb and arsenic concentrations between 10 ppb and 46 ppb, respectively. When non-drinking water sources are considered, they found that 20 out of 26 wells (76.92%) they studied had persistent elevated arsenic concentrations in 2021 based on their statistical analyses. They have recommended further continuous monitoring of water quality and arsenic mapping to be conducted in the province of Batangas to determine the extent of arsenic contamination of the groundwater. They have also recommended to provide alternative water supply for the affected communities. In addition to these, 9 out of 17 (52.94%) water treatment plant outlets and water sources were found to have arsenic concentrations ranging from 20 ppb to 70 ppb in the municipalities of Calauan, Bay, and Los Baños in the province of Laguna last September 2020, according to the 2020 Annual Audit Report on the Laguna Water District by the Commission on Audit (COA) [10]. Alarmingly, arsenic concentrations in the province of Laguna, especially in the municipalities of Bay and Los Baños, still have arsenic concentrations above the 10 ppb limit after two years, according to the 2022 Annual Audit Report on the Laguna Water District by COA [11]. On the same annual audit report, a 30-day trial was conducted to reduce the arsenic concentrations at Lopez Heights Pumping Station below the 10 ppb limit last October 10, 2022; however, the trial failed, and all groundwater sources contaminated with high amounts of arsenic is being considered to be shut down since the proposed solution of using reverse osmosis to remove arsenic incurs high capital expenditure.

Within the three provinces, arsenic contamination of groundwater hinders the availability of cheap and affordable water supply. It threatens human health, which impedes the achievement of SDG 3, SDG 6, and SDG 11 for these communities. Arsenic is a naturally occurring element found in high concentrations in certain water sources and is classified as a Group 1 human carcinogen by WHO

[12]. In addition, arsenic is also considered by the US Environmental Protection Agency (USEPA) and the Council of European Communities (CEC) as a prime pollutant [13]. Arsenic in drinking water can lead to arsenic poisoning or arsenicosis [12, 14]. Generally, arsenic contamination in surface water is less than in groundwater, and surface water is contaminated mainly due to anthropogenic activities, while groundwater contamination is primarily by natural sources [12].

Electrochemical Arsenic Remediation (ECAR) is one method that removes arsenic in water. ECAR produces coagulants in situ through electrocoagulation to remove arsenic in groundwater [12, 14, 15]. Electrocoagulation is becoming more prominent due to its rapid and effective removal of arsenic from water [13]. It is also deemed environmentally friendly compared with chemical coagulation and produces lower quantity, stable sludge [12, 13, 14, 16]. Unlike conventional methods, electrocoagulation is low-cost and is easy to implement, operate, and maintain with locally available materials. Electrocoagulation also does not introduce undesirable anions like chemical coagulation [17].

The arsenic removal efficiency of electrocoagulation is higher than that of conventional chemical coagulation. Iron electrocoagulation can remove greater than 95%-99% of arsenic from the water [12]. This range of arsenic removal efficiencies is proven by a study done by the University of California Berkeley (UC Berkeley) in Bangladesh, where they showed that iron electrocoagulation technology was able to reduce the arsenic content of both synthetic and natural groundwater from 3000 ppb to 10 ppb, which is within the WHO acceptable level [14].

The arsenic removal efficiency of ECAR depends on a lot of factors. These factors include pH [18], dissolved oxygen [16, 19], and ions such as phosphates [12, 13, 20], calcium, and magnesium [15, 17]. These factors should be considered for the efficient removal of arsenic in water.

According to Amrose et al. [21], Dutta & Gupta [22], and Kobya et al. [23], charge loading is a crucial factor in ECAR since it controls the production rate of coagulants which affects arsenic removal rate and increasing charge loading generally results in higher arsenic removal rate. It should be noted, however, that excessive charge loading can hinder floc flotation and separation due to high charge density and poor affinity between hydroxide flocs and gas bubbles [23]. Additionally, excessive charge loading results in higher energy costs and, with prolonged use and high charge loading cycles, results in the formation of a passivation layer on the electrodes which can increase power requirements over time, impacting the long-term operational costs of ECAR [23, 24].

Van Genuchten et al. [15] found that bivalent cations (e.g., calcium(II) and magnesium(II)) improve arsenic removal by (1) enhancing oxyanion adsorption, (2) promoting crystallite aggregation and (3) altering precipitate mineral phase and primary crystallite size. This contrasts oxyanions that reduce precipitate crystallite size, resulting in stable colloidal suspensions. Their study also suggests calcium(II) has stronger interactions with oxyanions than magnesium(II). Oxyanion interaction of both calcium(II) and magnesium(II) are arranged in the following from strongest to weakest: phosphates> arsenic(V) > silicates. Van Genuchten et al. [25] also reported that calcium(II) specifically acts as a catalyst for interparticle bridging of iron-arsenic complexes and iron-phosphate complexes.

Catrouillet et al. [26] investigated the mechanism of arsenic removal in the presence of manganese(Mn) in water of different pH. At pH 4.5, they found out that arsenic(III) was rapidly oxidized by hydroxyl radicals(OH•), and manganese-enhanced the aggregation of arsenic(V)-iron(III) polymers. On the other hand, they found that manganese(II) and arsenic(III) compete for iron(IV) at pH 8.5, which results in arsenic(III) remaining in the solution. Arsenic(V) that formed at pH 8.5 is incorporated into the structure of arsenic(V)-iron(III) polymers and ferrihydrite-like phases that contained 8% manganese(III) and adsorbed some arsenic(III). Catrouillet et al. [26] also noted that arsenic(III) and manganese(II) compete for the oxidants at intermediate pH values (~ pH 6.5); however, manganese(III) behaved as a reactive intermediate that reacted with iron(II) or arsenic(III) which explains the presence of arsenic(V) in the precipitates.

Understanding the factors affecting arsenic removal in electrocoagulation, especially those with limited studies such as cations, is essential as this helps predict the performance of ECAR and allows better optimization of parameters for operational implementation. Both studies conducted by Catrouillet et al. [26] and Van Genuchten et al. [15] are among the few studies investigating cations' effects on arsenic removal during electrocoagulation. Both studies examined the mechanisms and reactions involved in arsenic removal in the presence of calcium or manganese. However, neither of these studies incorporated rigorous statistical analyses that could quantitatively demonstrate whether the observed effects of cations in arsenic removal in their experiments were statistically significant. Additionally, low charge loading has been used by different studies such as those conducted by Kobya et al. [23] where they investigated the effects of 1-130 C/L charge loading on 75-500 ppb arsenic, by Dutta et al. [22] where they find the optimal charge loading from 5-30 C/L with 60-110 ppb arsenic, and by Dutta and Gupta [27] where they find the optimal charge loading from 5-120 C/L with 200 ppb arsenic and activated alumina after ECAR. However, these studies use a direct power source with no reported reference electrode to ensure constant charge loading and mostly used high charge loading on high arsenic concentrations. In this study, the effect of manganese(II) on arsenic removal in electrocoagulation at a low charge loading rate (5 C/L) and low arsenic concentrations mimicking real-world concentrations was investigated and quantified using regression analysis. This research aims to support SDGs 3, 6, and 11 by promoting technologies that could help in producing safe and clean water to protect the health and well-being of everyone residing in cities and communities with the following objectives:

1. determine the removal of arsenic using Electrochemical Arsenic Remediation (ECAR) in contaminated water (spiked solution) with and without manganese(II);
2. investigate the effect of manganese(II) on the removal of arsenic in contaminated water (spiked solution) using ECAR; and
3. verify the significant factors and estimate marginal effects in ECAR using the Generalized Additive Model (GAM).

2 Methodology

2.1 Preparation of Materials

The preparation of materials in this study was based on van Genuchten et al. [25]. All glassware used in the experiment was washed using a 1% nitric acid (HNO_3) bath and then washed with ultrapure 18.2 M Ω deionized water before air drying. Iron electrodes were soaked in 10% hydrochloric acid (HCl) solution for 20 minutes. Iron electrodes were then washed with copious running water. Rust and other particles were removed using steel wool and then with fine sandpaper. Iron electrodes were then stored in a desiccator with silica gel. The appearance of iron electrodes after cleaning is shown in Figure 1.

Analytical grade sodium arsenite ($NaAsO_2$), manganese(II) sulfate ($MnSO_4$), and ultrapure 18.2 Ω deionized water were used to prepare 250 mL of 20 parts per million (ppm) arsenic(III) and 250 mL of 500 ppm manganese(II) stock solution. Two liters of 20 ppb, 40 ppb, and 100 ppb arsenic(III) solution were prepared for the control setup. Two liters of solution with 20 ppb arsenic(III) + 500 ppb manganese(II) and 120 ppb arsenic(III) + 500 ppb manganese(II) were prepared for the arsenic-manganese combination setup.

2.2 ECAR Experiment

The electrocoagulation setup of the experiment was also based on van Genuchten et al. [25]. Figure 2 shows the configuration of the electrocoagulation setup used in this experiment. Before each run, Fe electrodes were washed with ultrapure 18.2 Ω deionized water and were only used once. Silver/silver chloride (Ag/AgCl) reference electrode was used and washed with ultrapure 18.2 Ω

Figure 1.
Fe electrodes after electrode cleaning

deionized water before each run. An Ag/AgCl electrode was used as a reference electrode to ensure a fixed charge loading of 5 C/L was applied to the solutions. A reference electrode provides a well-defined and stable reference potential. Electrode spacing was ~5 cm. The anode and cathode were arranged to have approximately the same submerged area (~13-14 cm^2).

Each setup has 500 mL of the solution and was run with a charge loading of 5 C/L for 30 minutes (0.17 C/L-min dosage rate) using potentiostat. Each experiment setup is run twice and sampled thrice for measurement. Samples were filtered using 0.22 μm filter paper and analyzed using inductively coupled plasma atomic emission spectroscopy (ICP-AES) from Teledyne. The pH of each setup was also measured before and after electrocoagulation using pH paper.

2.3 Statistical Analysis

The statistical significance of the initial arsenic and manganese concentrations on the final arsenic concentration was determined using R and R Studio for regression analysis. Correlation analysis was conducted using the “ggpairs” function from the “GGally" package developed by Schloerke et al. [28]. Generalized additive models (GAM) were used by using the “gam” function from the “mgcv” package developed by Wood [29] to model the relationships of the variables in the data.

In many studies, GAMs have already been used to investigate relationships between variables. For instance, Liu et al. [30] used GAMs to analyze the interactive effects of different water quality

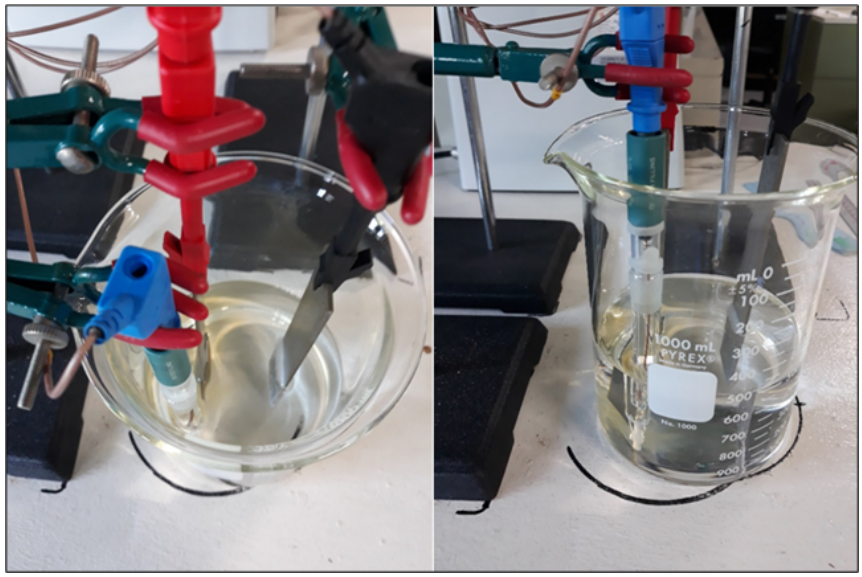

Figure 2.
ECAR setup. The anode is the red terminal, the cathode is the black terminal, and the $Ag/AgCl$ electrode is the blue terminal.

parameters on the water purification of a deep oxidation pond with horizontal subsurface flow constructed wetland. On the other hand, Liu et al. [31], on the other hand, examined the interactions between different water quality parameters and the removal efficiency of sulfamethoxazole in an electrolysis-integrated tidal flow-constructed wetland system. Further, Amin et al. [32] used GAMs to determine the impact of various factors on carbon dioxide emissions in Bangladesh, Ye et al. [33] applied GAMs to assess the impact of multiple factors on heavy metal leaching from nickel tailings, and Marques et al. [34] assessed potential biomarkers of contaminants in estuaries using biochemical and physiological parameters in croakers (*Micropogonias furnieri*) with GAMs.

The following is the formulation of the GAM used in this study:

```
arsenic_final_concentration ~
s(manganese_initial_concentration, k = 3) +
s(arsenic_initial_concentration, k = 3) +
ti(manganese_initial\_concentration,
arsenic_initial_concentration, k = 3)
```

The “s()” wrapped around the variables means that the variables are modeled using smooth terms and the “ti()” wrapped around the two variables means that the variables are modeled as tensor product interactions. The basis dimensions (k) for all terms are set to equal three to avoid overfitting due to the limited number of measurement data used in the GAM (n=27). Basis functions are additively combined to create smooth terms, as discussed by Wood [35]. Setting the basis dimension to three means that the basis functions can only have degree two (k-1) complexity, i.e., the basis functions are only limited to quadratic functions at most.

The average estimated marginal effects of initial arsenic concentration and initial manganese concentration to the final arsenic concentration were also calculated using the “slopes()” function of the “marginal effects” package developed by Arel-Bundock et al. [36]. Marginal effects were estimated at 0 ppb, 400 ppb, 450 ppb, 500 ppb, and 550 ppb of initial manganese concentrations while marginal effects of initial arsenic concentration were estimated at 10 ppb, 20 ppb, 30 ppb, 40 ppb, 80 ppb, 100 ppb, and 120 ppb. Intermediate concentration values were also included in the estimation of marginal effects to capture the inherent variability between raw concentration values

of arsenic and manganese and to help quantify how the effects of the initial arsenic and manganese concentration on the final arsenic concentration changes as their concentration increases.

3 Results and Discussion

3.1 ECAR Experiments

Arsenic is removed during the electrocoagulation via the following mechanisms. Electric current is passed through iron electrodes and iron(II) is then dissolved, which in the presence of dissolved oxygen, gets oxidized into iron(III) [19, 20]. Iron(III) ions polymerize to produce reactive iron(III) (oxyhydr)oxides that bind to arsenic(V) [19]. If arsenic(V) is present, iron(III)-arsenic precipitates and complexes are formed; thus, arsenic gets removed by the separation of the precipitates and complexes from the solution through gravitational settling and/or filtration [19, 20].

During oxidation by dissolved oxygen, iron(II) can also form a highly reactive iron(IV) oxidant, which can oxidize arsenic(III) into arsenic(IV) [20]. If enough iron(IV) is present, iron(IV) may further oxidize arsenic(IV) to arsenic(V), which then adsorbs iron(III) and precipitates from the solution [16, 20].

Hydrogen gas also forms in the cathode during electrocoagulation [12, 13, 19]. Hydrogen gas may remove flocs that never settle through gravitation by taking the flocs at the top of the solution (also called electro-floatation), forming a foam-like phase at the top of the solution, which can be removed by skimming [12, 13]. The flocs formed are usually negatively charged [12].

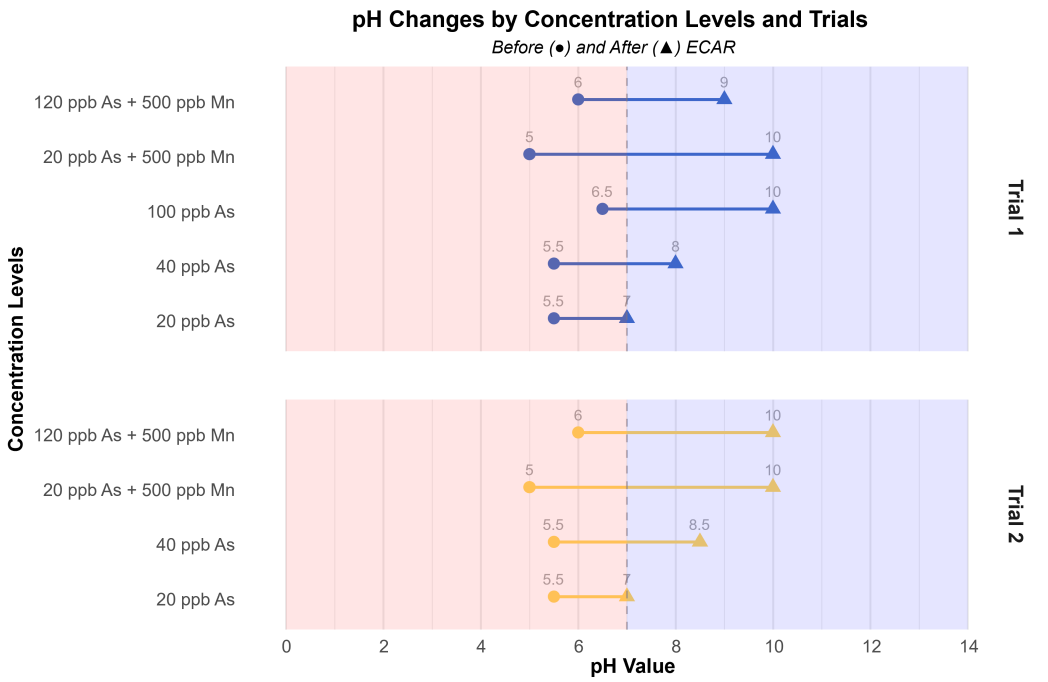

Figure 3.
pH of control setup before and after ECAR

The pH value of both the control and arsenic-manganese setup increased after ECAR from acidic to basic, as shown in Figure 3. This increase in pH is in agreement with Nidheesh and Singh [12] and Song et al. [13], as hydroxyl ions accumulate during electrolysis. All ECAR setups have also been observed to have yellowish to orangish color during and after electrocoagulation, as shown in Figure 4. The colors indicate the presence of lepidocrocite (γ-FeOOH) and/or goethite (α-FeOOH) as a predominant species of coagulant in electrocoagulation, as explained by Dubrawski et al. [37], Song et al. [13], and Wan et al. [18].

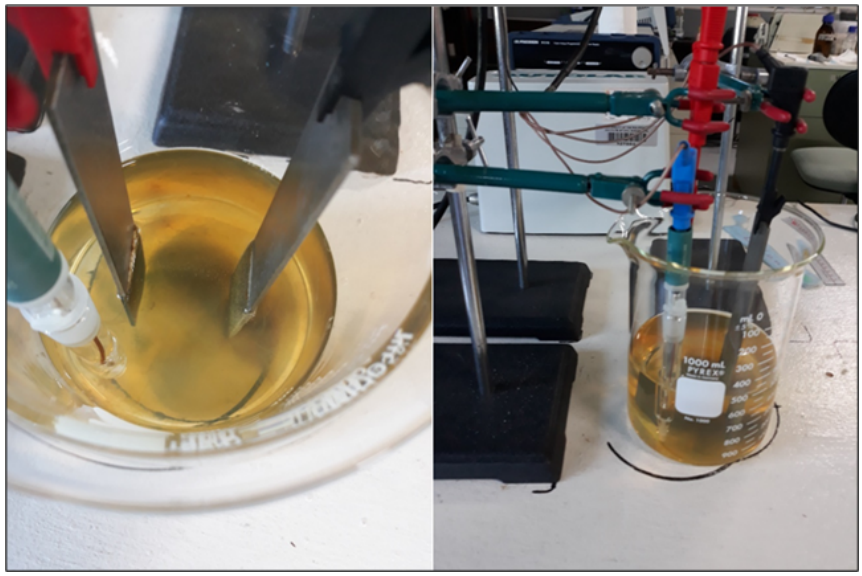

Figure 4.
Color of contaminated water (spiked solution) after ECAR

The mean arsenic percent removal of the control setup across concentration levels is about 76.78% while the mean arsenic percent removal of the arsenic-manganese setup is 97.59% across the concentration levels as shown in Figure 5. The raincloud plot – a combination of point plot, box plot, and violin plot – also illustrates that the measurements for arsenic percent removal greatly vary with a median of about 73.59%, while the arsenic percent removal of the arsenic-manganese setup aggregate around a single value (100%) which causes the box plot to be not visible and only to look a single line. Based on the aggregation of values in the arsenic-manganese setup, it could be seen that one measurement is an outlier which can be attributed to imprecise measurement as seen in Table 1 where the standard errors are large.

Table 1. Arsenic Removal of the Control Setup and Arsenic-Manganese Setup. Each trial consists of three measurements

	Trial	Theoretical As [ppb]	As Percent Removal	Theoretical Mn [ppb]	Mn Percent Removal
Control	1	20	96.89±5.38	—	—
	2	20	82.96±8.53	—	—
	1	40	71.04±4.69	—	—
	2	40	61.34±7.28	—	—
	1	100	71.68±1.76	—	—
As-Mn	1	20	90.34±16.74	500	100.00*
	2	20	100.00*	500	100.00*
	1	120	100.00*	500	100.00*
	2	120	100.00*	500	100.00*

zero standard deviation

Arsenic removal in the control setup is between 61%-96% and large variability of arsenic percent removal for each trial, especially for the second trial, is also observed as seen in Figure 6. This large variability in the measurement of arsenic percent removal can be attributed to the low concentrations used in the experiments. Despite the variability in measurements, arsenic percent removal generally decreases as the initial concentration of arsenic increases. This trend is expected since the charge loading of the setup was held constant at 5 C/L. Thus, the generation rate of coagulants

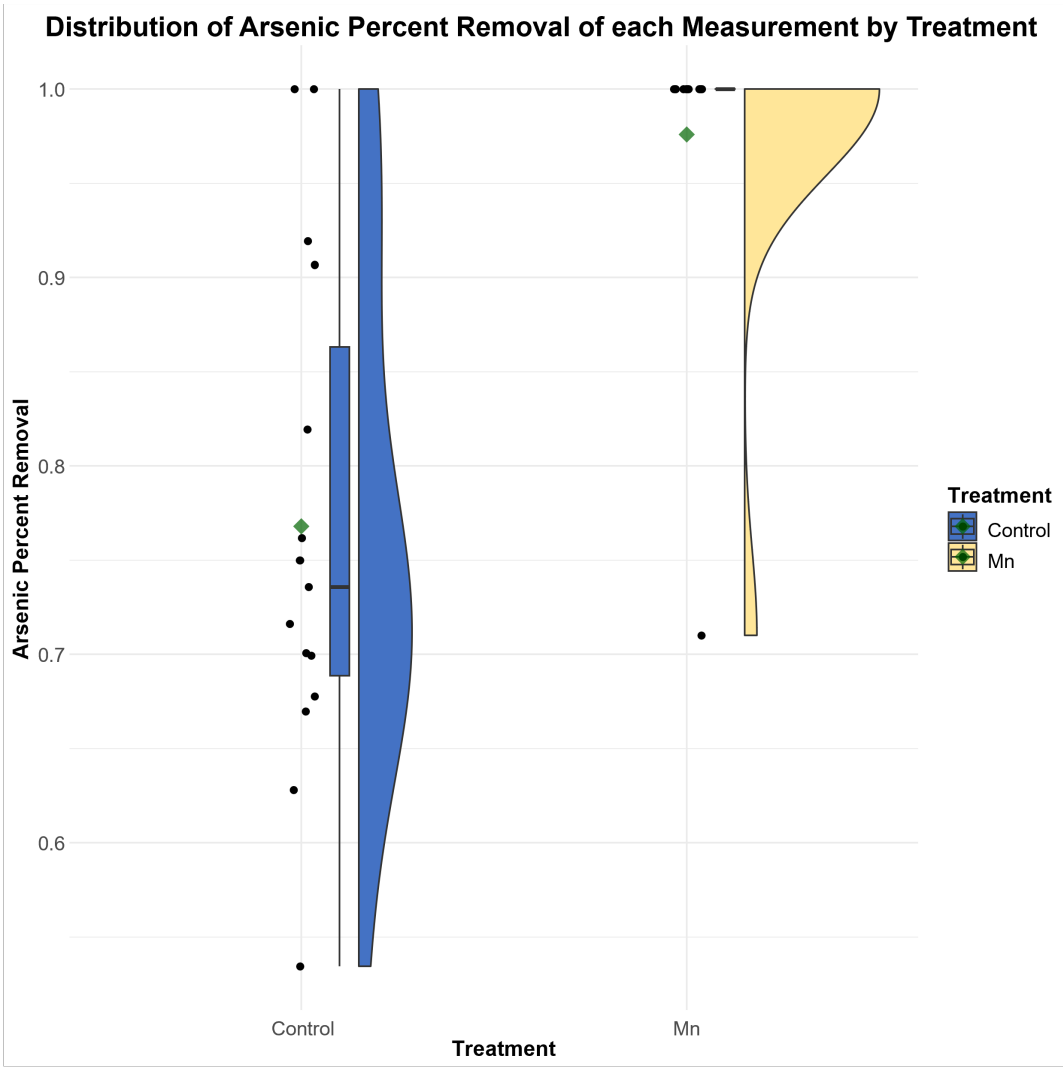

Figure 5.
Distribution of Arsenic Percent Removal of Control and As-Mn. The green diamond point indicates the mean

is constant. This means that the constant amount of coagulants is not enough to precipitate arsenic at higher concentrations. Overall, ECAR at a charge loading of 5 C/L of the control setup is only compliant with the maximum 10 ppb arsenic concentration set by WHO and DOH when the initial arsenic concentration is 20 ppb.

For the arsenic-manganese setup, arsenic removal is mostly 100% with no variability aside from a single outlier as shown in Figure 7. As discussed previously, the outlier can be attributed to imprecise measurement. Despite the outlier with a final arsenic concentration of 6.66 ppb, final arsenic concentrations in all setups of arsenic-manganese solutions are below the maximum 10 ppb arsenic concentration set by WHO and DOH. Results of these experiments suggest that manganese(II) helps remove arsenic in water at pH 5 to pH 6, which agrees with the results of Catrouillet et al. [26] at pH 4.5.

The charge loading rate is given by the following equation from Amrose et al. [22]:

$$q = \frac{I * t_e}{V} \quad (1)$$

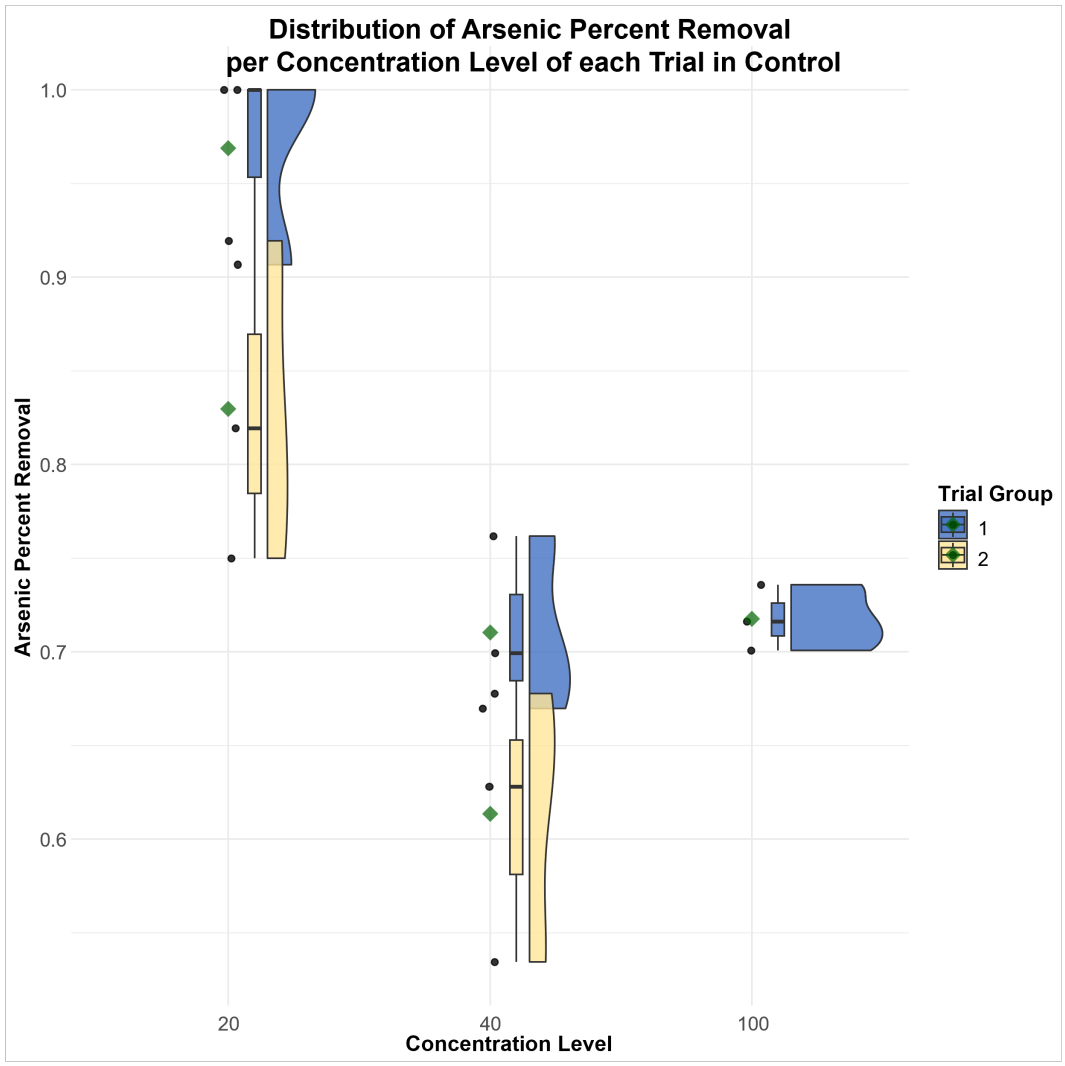

Figure 6.
Distribution of Arsenic Percent Removal of Control and As-Mn. The green diamond point indicates the mean

where q is the charge loading rate (C/L), I is the constant operating current (C/s or A), t_e is the electrolysis time, and V is the solution volume (L). Using Equation (1), the charge loading rate used by Catrouillet et al. [26] is calculated to be 46.08 C/L, whereas this study uses 5 C/L. Despite the vast difference (9̃×) in charge loading rates, the results of this study still validate the findings of Catrouillet et al. [26], even at low charge loading rates where manganese enhanced the aggregation of arsenic(V)-iron(III) polymers at low pH regime (pH 4.5); thus, enhancing arsenic removal.

Results also show that manganese was 100% removed from the solution after ECAR, as presented in Table 1. This removal rate is in contrast to the results by Catrouillet et al. [26], where only 4.2% and 3.7% manganese removal after ECAR was observed for their 10 μM arsenic + 100 μM manganese setup and 100 μM arsenic + 100 μM manganese setup, respectively. Catrouillet et al. [26] used a 1:10 and 1:1 arsenic(III):manganese(II) ratio, while this study used 2:50 and 12:50. If the discrepancy between the manganese removal between the two studies might be due to the arsenic(III):manganese(II) ratio used, then the manganese removal of this study's 20 ppb arsenic + 500 ppb manganese setup should be lower than the 10 μM arsenic + 100 μM manganese setup by Catrouillet et al. [26], but this is not the case.

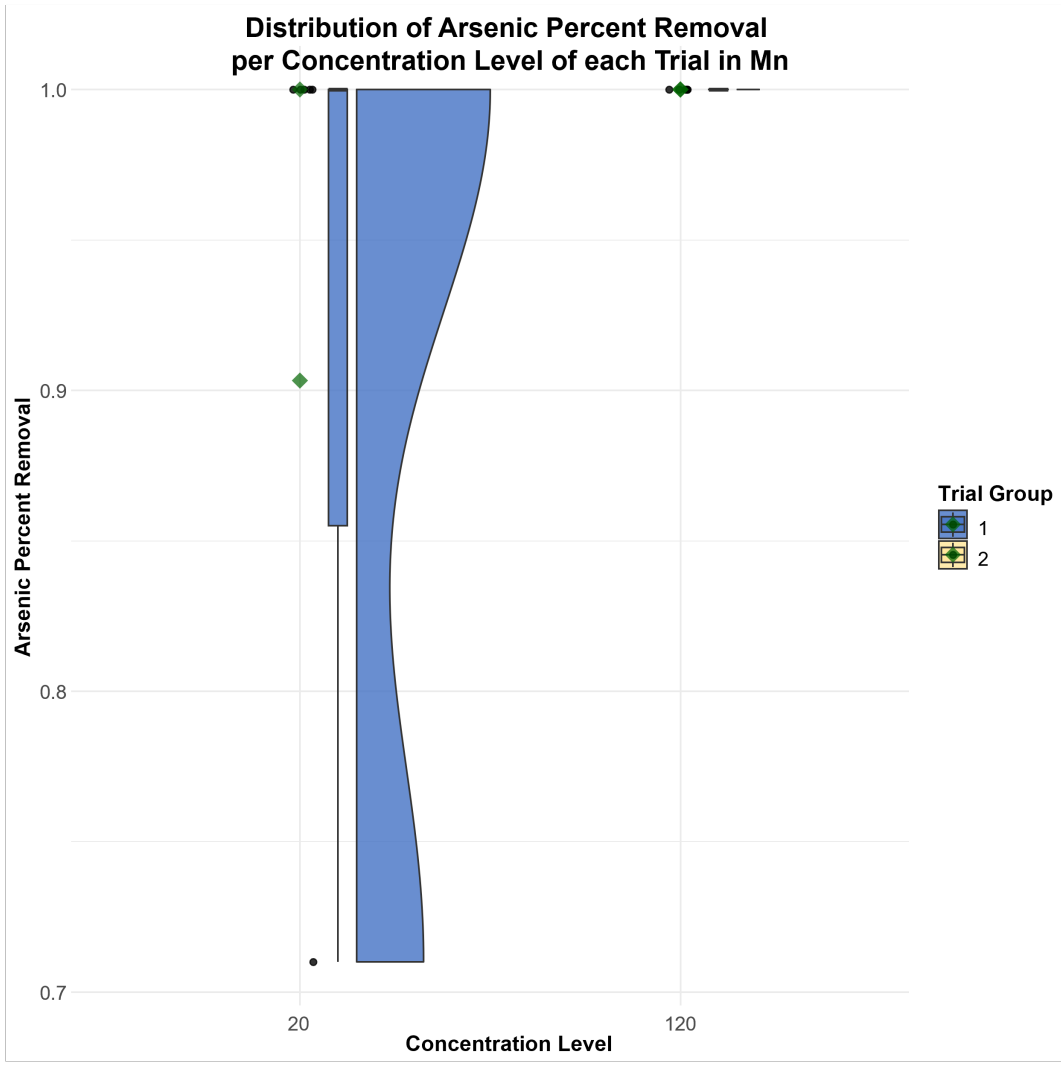

Figure 7.
Arsenic Percent Removal of the Control Setup per Concentration Level and Trial. Each trial consists of 3 measurements and the green diamond point represents the mean of each trial.

The theoretical amount of iron(II) generated in moles during electrocoagulation is given by the following equation from Catrouillet et al. [26]:

$$Fe = \frac{I * t_e}{n * F} \tag{2}$$

where I is the constant current (C/s), t_e is the electrolysis time (s), n is the number of transferred electrons (n=2, for iron(II)), and F is the Faraday's constant (96,485 C/mol). Using Equation (2), the iron(II) generated in this study is at a rate of 0.8637 μM/min, which is less than the 7 μM/min rate by Catrouillet et al. [26]. Based on these values, the arsenic(III):iron(II):manganese(II) ratio used in the study by Catrouillet et al. [26] is approximately 1:23:10 and 1:2:1, whereas this study has an arsenic(III):iron(II):manganese(II) ratio of around 2:145:50 and 12:145:50. Thus, it could be inferred that the complete removal of manganese in this study is due to the electrosynthesis of excess iron(II) and manganese(II) into manganese ferrite ($MnFe_2O_4$) nanoparticles as conducted by Mosivand & Kazeminezhad [38].

3.2 Statistical Analysis

Negative and moderate correlation between manganese concentration and arsenic concentration after ECAR was found to be significant based on the calculated Pearson correlation coefficient found on the upper triangular matrix of Figure 8 and based on the correlation strength rating given by Dancey & Reidy [39], while the correlation with remaining variable combinations is positive, weak, and insignificant. The figure's diagonal illustrates each variable's data distribution while the remaining lower triangular matrix shows the scatterplot of each variable combination.

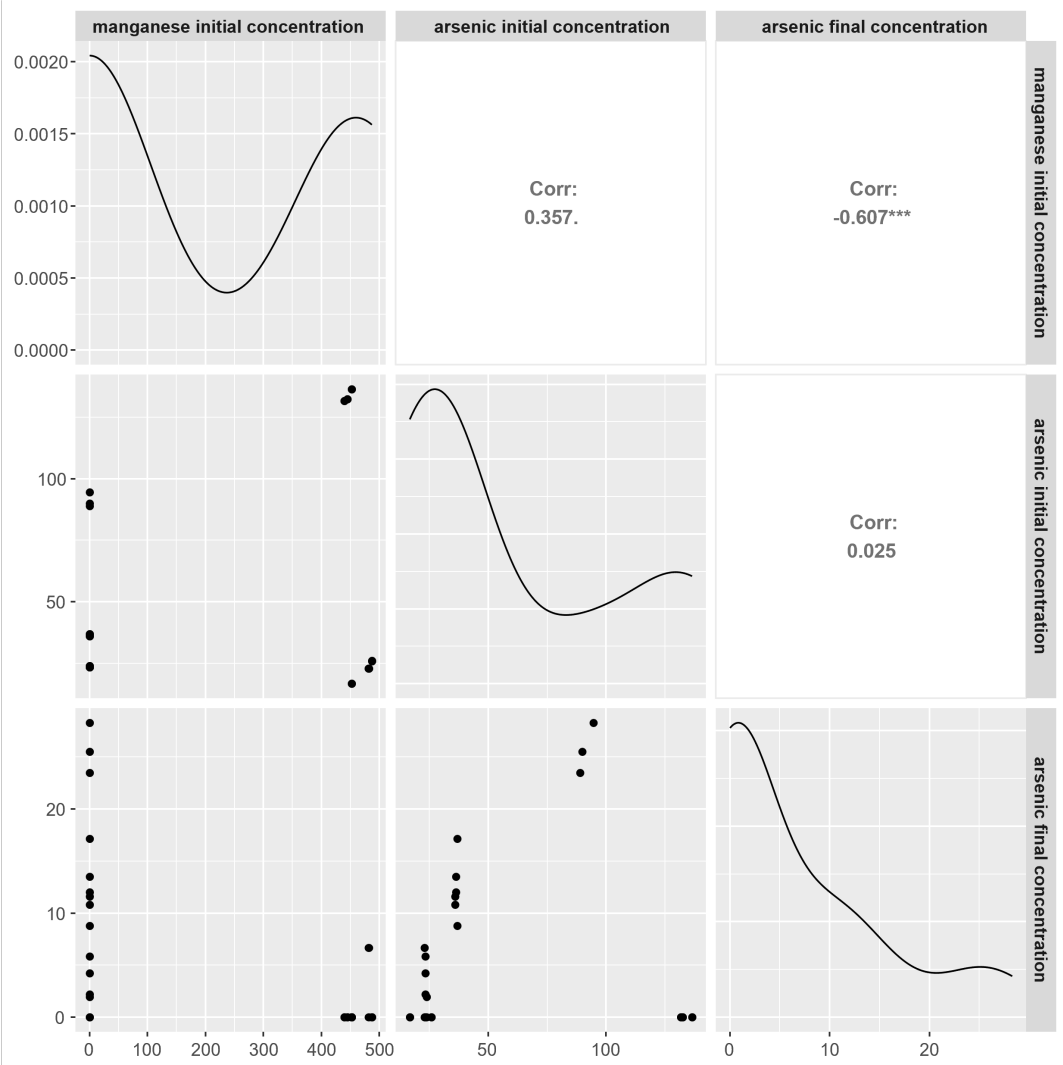

Figure 8.

Experiment Data Distribution and Correlation Plots. Significance Codes: ***significant at $\alpha = 0.001$, **significant at $\alpha = 0.01$, *significant at $\alpha = 0.05$, and "."significant at $\alpha = 0.1$.

Based on the generalized additive model, the effect of initial manganese concentration on the final arsenic concentration with an approximately linear relationship is significant as shown in Table 2 where the effective degrees of freedom (edf) of the smooth term [s(manganese initial concentration)] is equal to one and with p-value < 0.05.

p-values estimated by GAM are approximates and not a direct analog to the p-value reported by linear regression models. However, it is still safe to claim evidence of significance if the p-value calculated by the model is far enough from 0.05, which is the case for the GAM results. Additionally, edf values indicate the degree of smooth splines used by the model that are additively aggregated

Table 2. Generalized Additive Model Results

GAM Summary Statistics				
Parametric coefficients	**Estimate**	**Std. Error**	**t value**	**Pr(>|t|)**
(Intercept)	3.896	1.495	2.606	0.0166*
Approximate significance of smooth terms	**edf**	**Ref.df**	**F**	**p-value**
s(manganese initial concentration)	1	1	122.78	< 2.00E-16*
s(arsenic initial concentration)	1	1	11.34	0.00292*
ti(manganese initial concentration,arsenic initial concentration)	3.314	3.729	49.99	< 2.00E-16*
Model Fit				
Adjusted R-squared value	0.931			
Deviance Explained (R-squared value)	0.945			
***significant at α = 0.05**				

to model the relationship between variables, thus, higher edf values mean higher degree curves were used to model the relationship between the variables of interest.

GAM results also indicate the relationship between initial and final arsenic concentrations is approximately linear (stepwise linear) and significant. Interaction effects between initial arsenic concentration and initial manganese concentration were also significant, with at least a cubic relationship, as indicated by edf > 3. However, it is worth noting that there is concurvity between the main effects (initial manganese concentration, initial arsenic concentration) and interaction effects, thus, estimated interaction effects and their significance are unreliable. Nevertheless, the estimated interaction effects of GAM will still provide important insight into how each variable might affect each other.

Looking at the GAM diagnostic plots illustrated in Figure 9, it can be concluded that the GAM follows the assumptions necessary to draw insights from the modeling results correctly. Residuals are approximately distributed within the confidence band along the diagonal of the quantile-quantile plot (qq plot) with a few outliers at the end. Residuals are approximately symmetrical and roughly follow a normal distribution based on the histogram of residuals. In the residuals vs linear predictions plot, the residuals are approximately distributed around the zero-horizontal line without any clear pattern. Finally, the residuals in response vs fitted values plot roughly follows a 1:1 correspondence.

Partial effects plot of the initial manganese concentration, as shown in Figure 10, indicates that manganese has an approximately negative linear effect on the final arsenic concentration. Thus, we can conclude that manganese significantly helps decrease the concentration of arsenic in ECAR. Figure 11, on the other hand, shows the partial effects plot of the initial arsenic concentration to the final arsenic concentration, where an approximately positive relationship can be observed. This relationship is expected since the charge loading was held constant, which means the iron coagulants generated are insufficient to precipitate the increasing initial arsenic concentration. Some individual measurements fall outside the confidence bands of the partial effects plot of initial arsenic concentration and initial manganese concentration on the final arsenic concentration due to the considerable variability of each measurement and because of the small sample size (n = 27) used for the GAM. For example, the confidence band in the 100 to 120 range on the x-axis of the partial plot of initial arsenic concentration on the final arsenic concentration is wider due to the small samples or measurements conducted in that range. Nevertheless, the general trend and

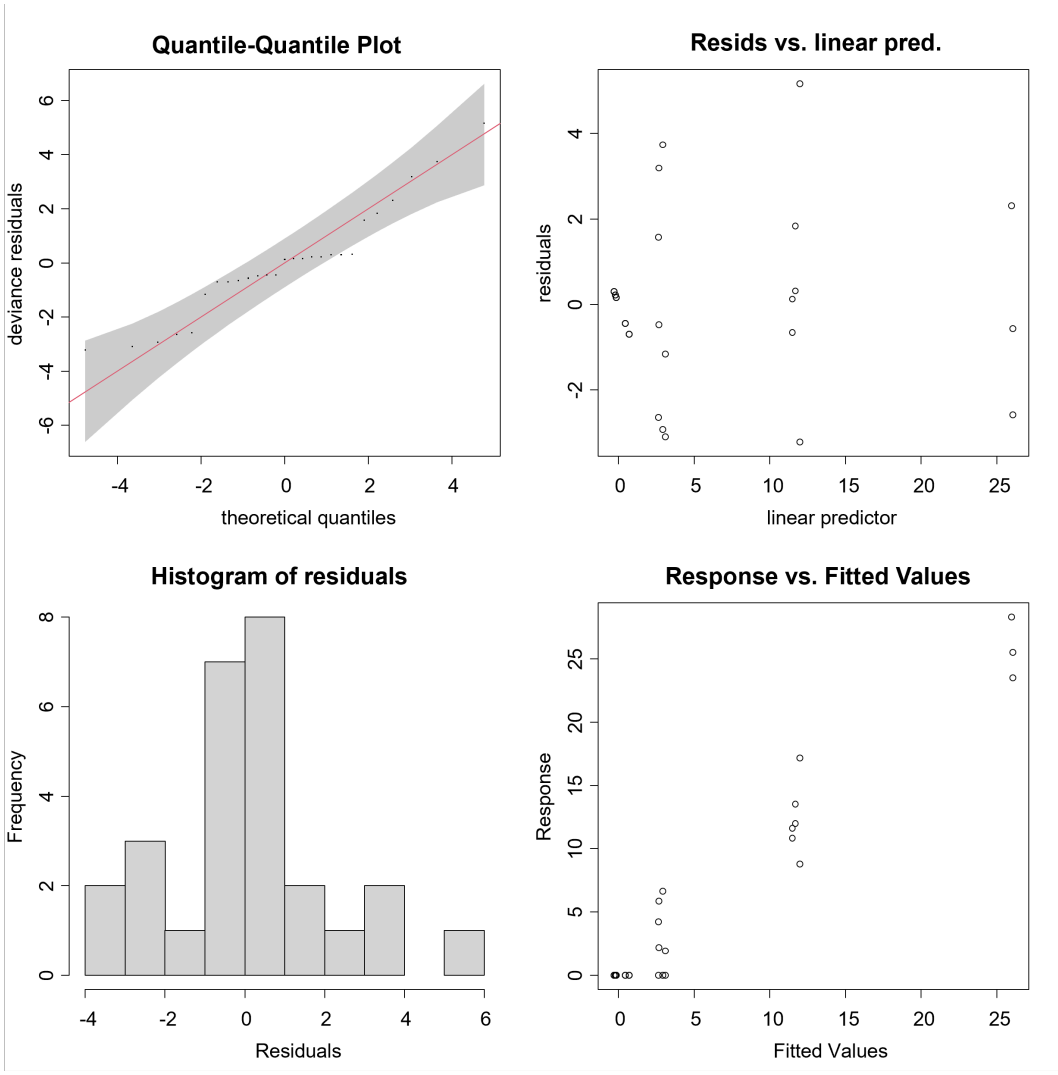

Figure 9.
GAM Diagnostic Plots

relationship in both the partial effects plots are still valid.

Partial effects plot of the interaction of initial arsenic concentration and initial manganese concentration on the final arsenic concentration is illustrated in Figure 12 where the interaction effects are only found in 4 regions representing the different concentration combinations of initial arsenic concentration and initial manganese concentration with their corresponding standard error. Figure 13, on the other hand, displays a heatmap of interaction of initial arsenic concentration and initial manganese concentration on the final arsenic concentration where the color ranges from red to yellow, corresponding to negative interaction effect (red) to positive interaction effect (yellow).

Based on these interaction effects plots, the concentration combination of 120 ppb arsenic and 500 ppb manganese, and 20 ppb arsenic only helps reduce the final arsenic concentration. Surprisingly, the interaction effects plots show that a combination of 20 ppb arsenic and 500 ppb manganese increases the final arsenic concentration which is different from the measurements where 100% arsenic removal was observed. This incorrect interaction result may be due to the concurvity present between the main effects and interaction effects and due to the small sample or measurement present on those variable concentration combinations. Interpolated and extrapolated effects of initial arsenic concentration and initial manganese concentration on the

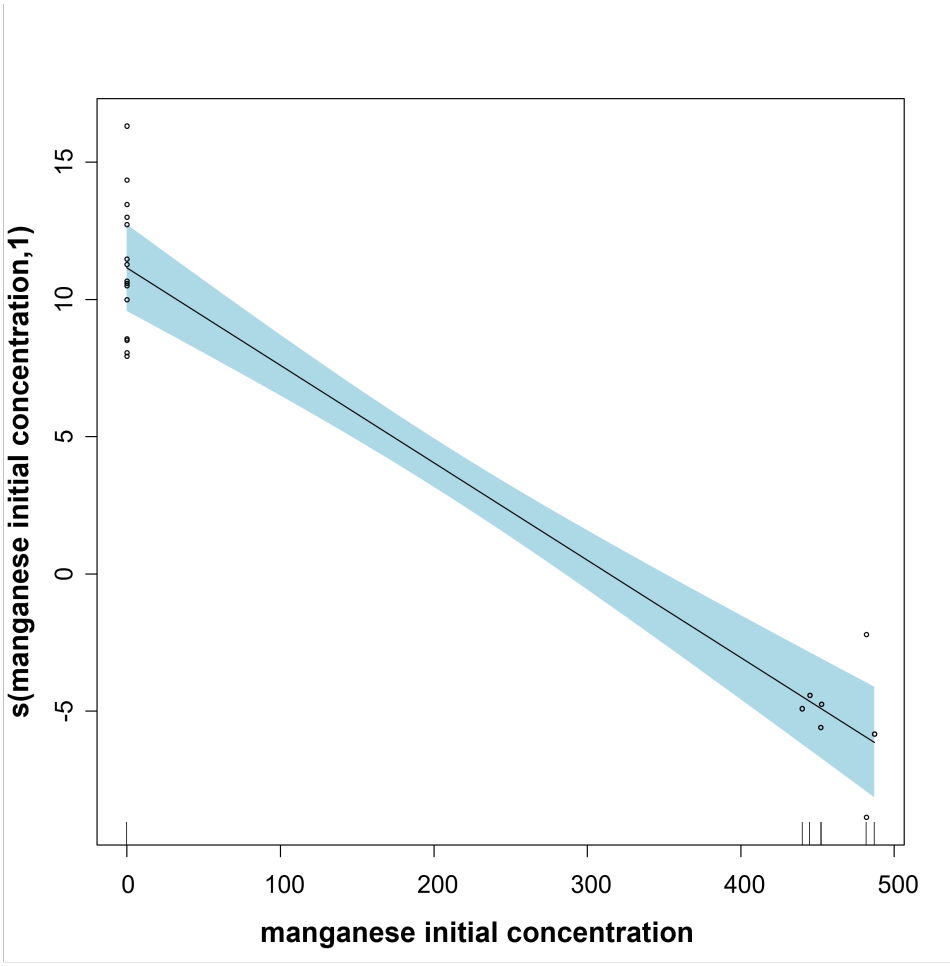

Figure 10.
Partial Effects of Initial Manganese Concentration on Final Arsenic Concentration

final arsenic concentration across a continuous range of concentration values are shown in Figure 14. Incorrect estimated effects on the final arsenic concentration can still be seen in the figure, especially in areas without experimental data for other variable concentration combinations. This reflects that the data used in the modeling is inadequate to estimate values in those intermediate regions correctly.

Estimated marginal effects of initial manganese concentrations and initial arsenic concentrations on the final arsenic concentration are illustrated in Table 3 and Table 4 respectively. Marginal effects are defined by Arel-Bundock et al. [36] as "partial derivatives of the regression equation with respect to a predictor of interest" and means that the estimated marginal effects are slopes tangent to the dependent variable to a particular value of the independent variable of interest. Thus, they caution that the estimated marginal effect must be seen as an approximation and only valid in a small neighborhood of the specific value of the independent variable of interest where the marginal effect is estimated and only in tiny increments or decrements. Due to these constraints, marginal effects were also estimated on intermediate concentration values of initial manganese concentrations and initial arsenic concentrations to help quantify how the effects of the initial arsenic and manganese concentration on the final arsenic concentration generally change as their concentration increases.

The estimated marginal effect of initial manganese concentrations on the final arsenic concentration is negative for all positive values of initial manganese concentrations, which aligns with the

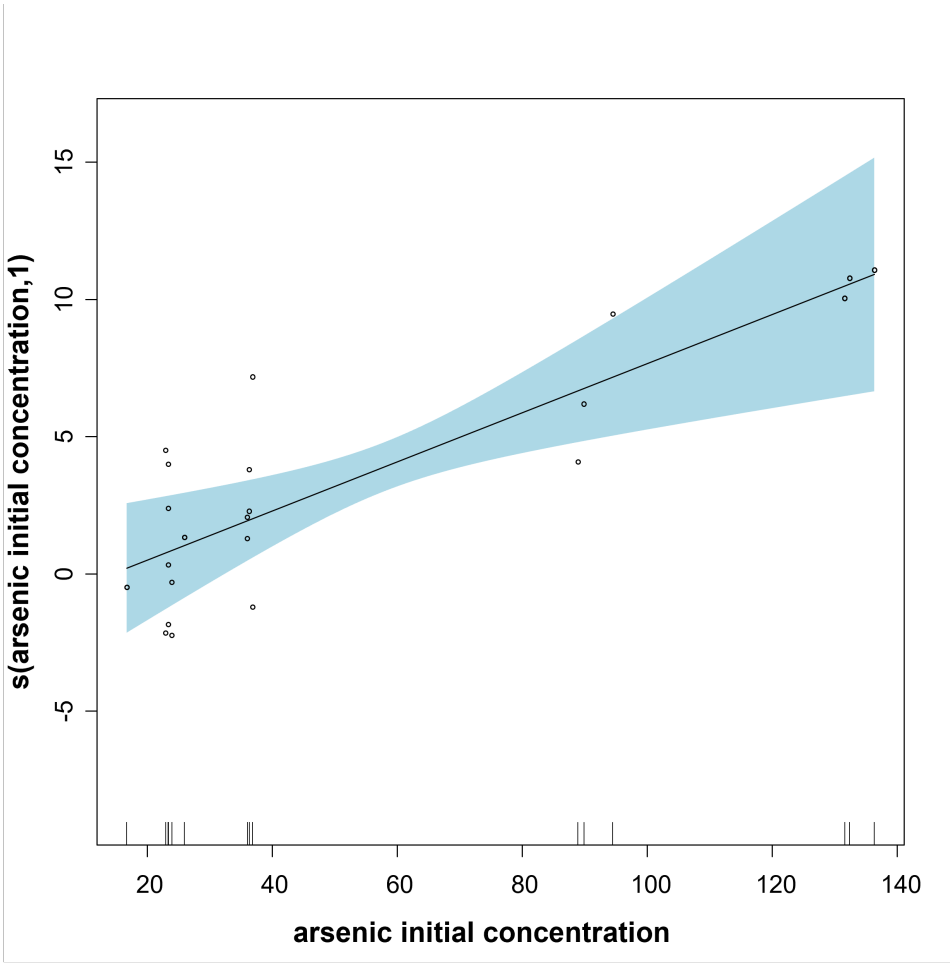

Figure 11.
Partial Effects of Initial Arsenic Concentration on Final Arsenic Concentration

partial dependence plot illustrated in Figure 10. By taking the average of the significant estimated marginal effect, the average estimated marginal effect of initial manganese concentrations on the final arsenic concentration is -0.4078, which means that we expect a decrease in the final arsenic concentration by 0.4078 ppb for each unit increase of initial manganese concentration as long as the unit increase is small.

The estimated marginal effect of initial arsenic concentrations on the final arsenic concentration is generally positive except at 100 ppb and 120 ppb arsenic, in which the estimated marginal effects are negative and insignificant. These exceptions can be explained by the lack of data for the GAM, as shown in the wide confidence band in the 100 ppb and 120 ppb range of the partial dependence plot shown in Figure 11.

Nevertheless, by only considering the significant estimated marginal effects, we can see that the estimated marginal effect of initial arsenic concentrations on the final arsenic concentration is in accordance with the partial dependence plot of initial arsenic concentration on the final arsenic concentration. By taking the average of the significant estimated marginal effect, the average estimated marginal effect of initial arsenic concentration on the final arsenic concentration is 1.778, which means that we expect an increase in the final arsenic concentration by 1.778 ppb for each unit increase of the initial arsenic concentration as long as the unit increase is small.

Based on the average estimated marginal effects of initial manganese concentrations and initial arsenic concentrations on the final arsenic concentration, we can see that the presence of

Table 3. Estimated Marginal Effect of Initial Manganese Concentration on Final Arsenic Concentration

Initial Manganese Concentration	Estimate	Std. Error	z	Pr(>|z|)	2.50%	97.50%
0	0.0879	0.102	0.859	0.3902	-0.113	0.2885
400	-0.3071	0.130	-2.366	0.0180*	-0.5620	-0.0527
450	-0.4121	0.191	-2.159	0.0308*	-0.7860	-0.0380
500	-0.4559	0.216	-2.107	0.0351*	-0.8800	-0.0319
550	-0.4559	0.216	-2.107	0.0351*	-0.8800	-0.0318
Average Estimated Marginal Effect		-0.4078				

*significant at α = 0.05

Table 4. Estimated Marginal Effect of Initial Arsenic Concentration on Final Arsenic Concentration

Initial Arsenic Concentration	Estimate	Std. Error	z	Pr(>|z|)	2.50%	97.50%
10	1.9747	0.912	2.166	0.0303*	0.188	3.761
20	1.9629	0.905	2.169	0.0300*	0.190	3.736
30	1.7803	0.799	2.227	0.0259*	0.214	3.347
40	1.3941	0.578	2.413	0.01580*	0.262	2.526
80	0.0697	0.242	0.288	0.7732	-0.404	0.544
100	-0.3325	0.460	-0.723	0.4696	-1.234	0.569
120	-0.5612	0.590	-0.952	0.3411	-1.717	0.594
Average Estimated Marginal Effect		1.778				

*significant at α = 0.05

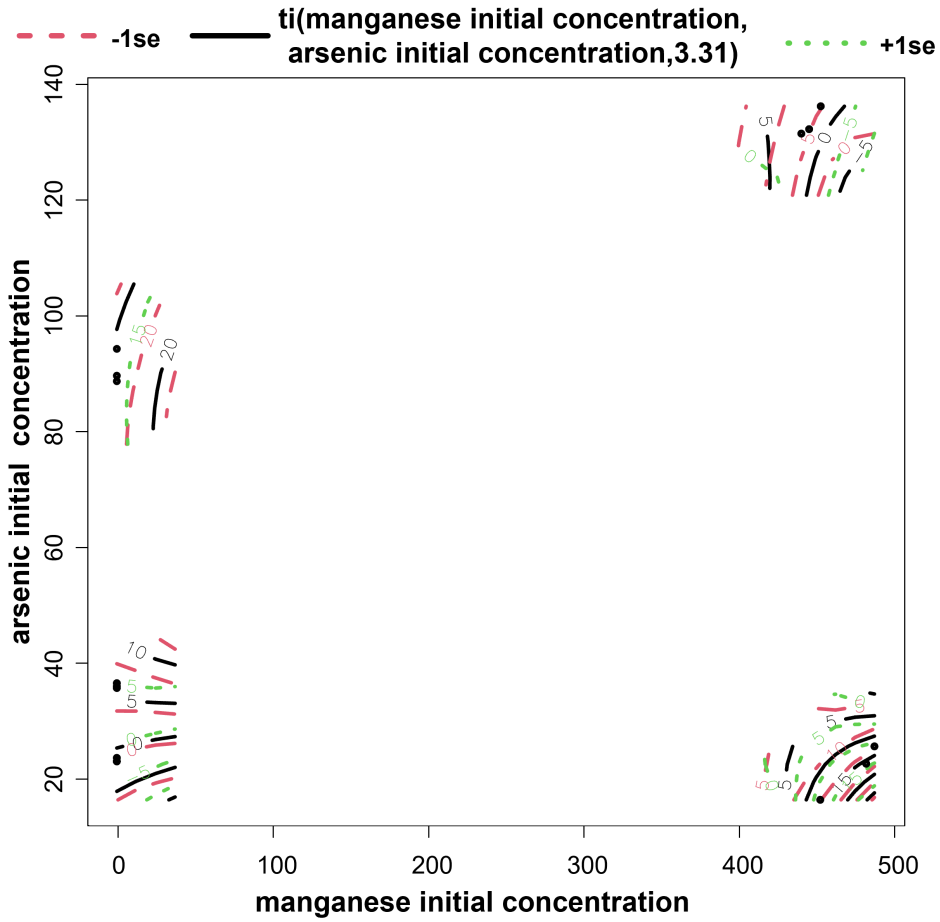

Figure 12.
Partial Effects of Initial Arsenic and Manganese Concentrations on the Final Arsenic Concentration. Red and green dashed lines indicate standard errors while the solid black line indicates the interaction effects estimated by the GAM.

manganese helps remove arsenic in ECAR. However, the effect of manganese is still small (about 4 times less) compared to the effect of initial arsenic concentration in arsenic removal.

4 Conclusion and Recommendations

Manganese was found to aid significantly arsenic removal mostly by 100% during ECAR with approximately 2:145:50 and 12:145:50 arsenic(III):iron(II):manganese(II) ratio at pH 5 to pH 6 and at a low charge loading rate of 5 C/L. Regardless of the arsenic-manganese solution setup, 500 ppb manganese reduced the arsenic concentration below the 10 ppb maximum arsenic concentration limit set by WHO and DOH for drinking water. Total removal of manganese after ECAR was also observed on all arsenic-manganese solutions, which may be due to the electrosynthesis of excess iron(II) and manganese(II) into manganese ferrite ($MnFe_2O_4$) nanoparticles.

Statistical analysis shows that the effects of initial arsenic and manganese concentrations and their interaction on the final arsenic concentration are significant. However, it should be noted that the significance of the interaction effects may be unreliable due to the concurvity between the interaction effects and the main effects. The average estimated marginal effect of initial arsenic and manganese concentrations on the final arsenic concentration is -0.40778 and 1.778 respectively.

The study shows that ECAR effectively removes arsenic from groundwater, particularly in the

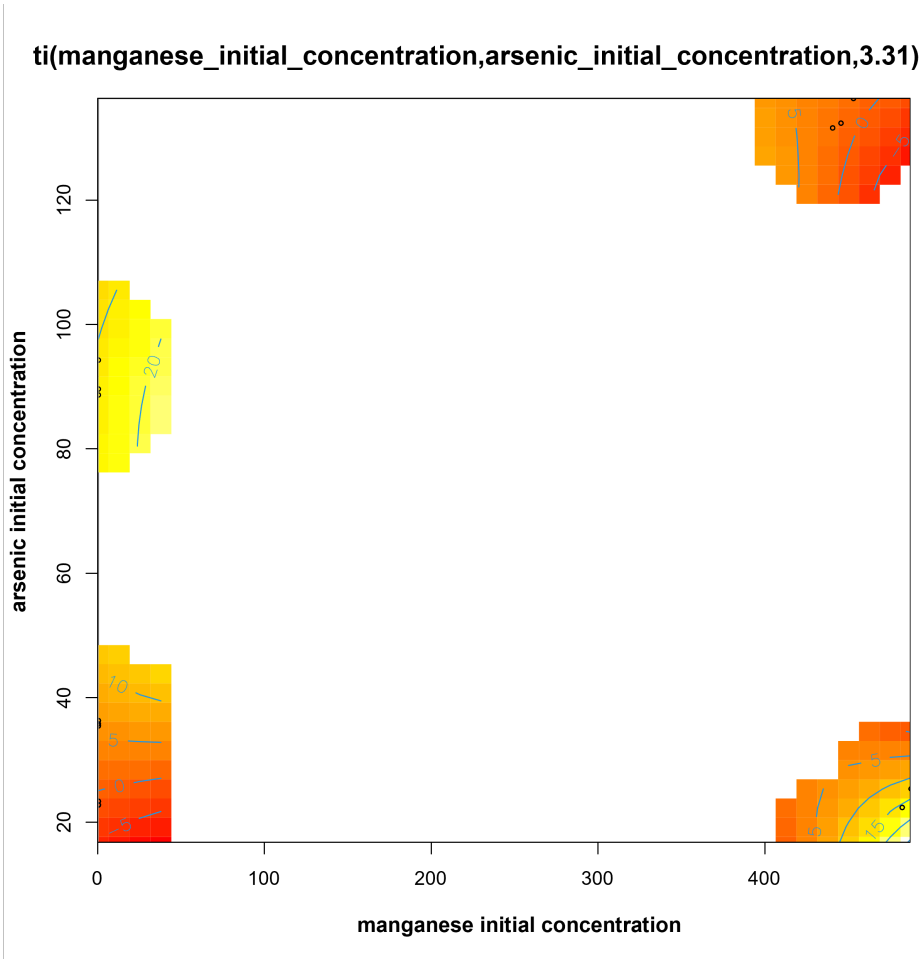

Figure 13.
Partial Effects Heatmap of Initial Arsenic and Manganese Concentrations on the Final Arsenic Concentration. The color ranges from red to yellow, corresponding to negative effect (red) to positive effect (yellow).

presence of manganese. This technology supports clean water access and aligns with three UN Sustainable Development Goals: health (SDG 3), clean water (SDG 6), and sustainable communities (SDG 11). However, it should be noted that the study is limited by the following:

1. the study used contaminated water (spiked solution) to determine the effect of manganese(II).
2. the study used only a fixed 5 C/L charge loading.
3. the study was conducted during the height of the pandemic which resulted in lockdowns; thus, not all planned trials were conducted.

To address these limitations, further investigation of the mechanism of total manganese removal after ECAR and further experiments with different arsenic(III):iron(II):manganese(II) ratios at various pH levels are recommended to elucidate further the interaction of arsenic, iron, and manganese in ECAR. For future research, the impact of additional factors, such as different charging times and charge loadings, diverse chemical ratios, and various metal impurities can be explored to simulate actual groundwater conditions. Finally, given the marginal effects observed in this study, future experiments should be designed and conducted with sufficient experiment trials and measurements to achieve appropriate statistical power.

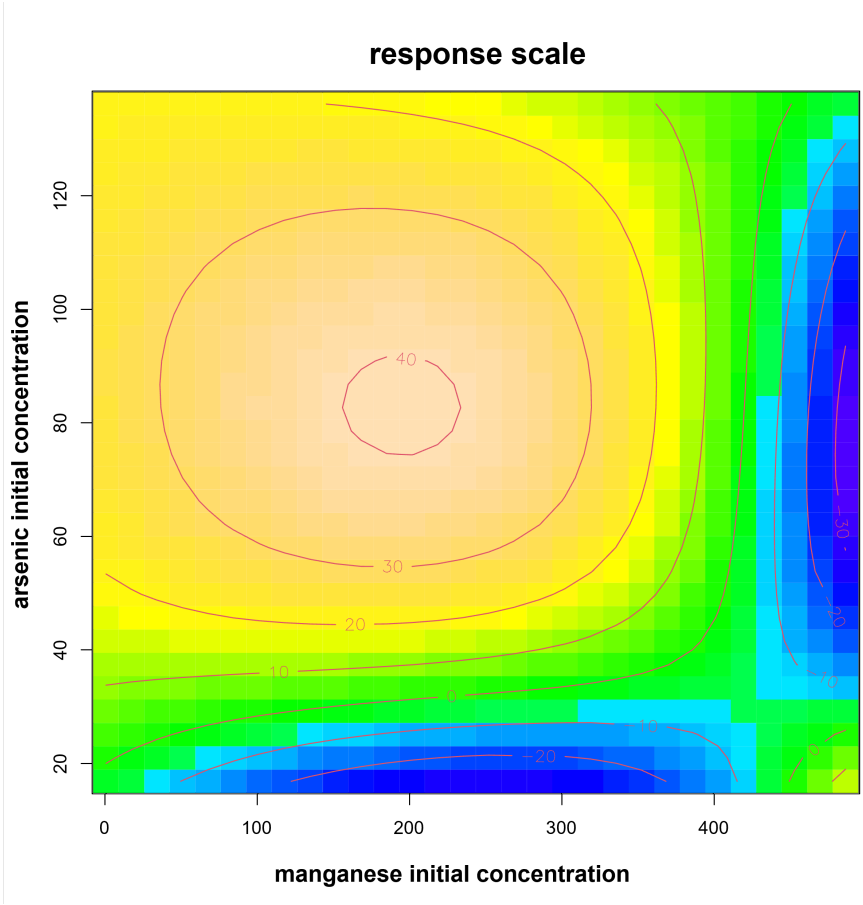

Figure 14.
Effects of Different Initial Concentrations of Arsenic and Manganese on Final Arsenic Concentration

Statements and Declarations

Funding Information

This study is under the Philippine Electrochemical Arsenic Remediation (PHIL-ECAR-I) Project funded by CHED-PCARI and implemented by the University of the Philippines Diliman.

Conflicts of Interest

The authors declare no conflict of interest.

Ethical Considerations

Not Applicable

Data Availability

The data in this study are available upon request from the authors.

Authors Contribution

A.K.B.R.: conceptualization, methodology, experimentation, statistical analysis, writing-major contribution and original draft preparation, **S.B.A.**: conceptualization, supervision, mentoring, writing-minor contribution, reviewing and editing of manuscript; **C.R.O.** and **A.C.R.**: conceptualization, funding, academic advising. All authors have read and agreed to the published version of the manuscript.

References

[1] United Nations. (2015). *Transforming our world: The 2030 agenda for sustainable development*. https://sdgs.un.org/sites/default/files/publications/21252030%20Agenda%20for%20Sustainable%20Development%20web.pdf

[2] Tortajada, C., & Biswas, A. K. (2018). Achieving universal access to clean water and sanitation in an era of water scarcity: Strengthening contributions from academia. *Current opinion in environmental sustainability*, *34*, 21–25. https://doi.org/10.1016/j.cosust.2018.08.001

[3] McDonald, R. I., Weber, K., Padowski, J., Flörke, M., Schneider, C., Green, P. A., Gleeson, T., Eckman, S., Lehner, B., Balk, D., et al. (2014). Water on an urban planet: Urbanization and the reach of urban water infrastructure. *Global environmental change*, *27*, 96–105. https://doi.org/10.1016/j.gloenvcha.2014.04.022

[4] Margat, J., & Van der Gun, J. (2013). *Groundwater around the world: A geographic synopsis*. Crc Press. https://doi.org/10.1201/b13977

[5] Husana, D. E., & Yamamuro, M. (2013). Groundwater quality in karst regions in the Philippines. *Limnology*, *14*, 293–299. https://doi.org/10.1007/s10201-013-0398-8

[6] Solis, K. L. B., Macasieb, R. Q., Parangat Jr, R. C., Resurreccion, A. C., & Ocon, J. D. (2020). Spatiotemporal variation of groundwater arsenic in Pampanga, Philippines. *Water*, *12*(9), 2366. https://doi.org/10.3390/w12092366

[7] World Health Organization. (2022). *Guidelines for drinking-water quality: Incorporating the first and second addenda*. https://www.who.int/publications/i/item/9789240045064

[8] Department of Health. (2017). *DOH Administrative Order No. 2017-0010: Philippine National Standards for Drinking Water*. https://www.fda.gov.ph/wp-content/uploads/2020/10/Administrative-Order-No.-2017-0010.pdf

[9] Apostol, G. L. C., Valenzuela, S., & Seposo, X. (2022). Arsenic in groundwater sources from selected communities surrounding Taal Volcano, Philippines: An exploratory study. *Earth*, *3*(1), 448–459. https://doi.org/10.3390/earth3010027

[10] Commission on Audit. (2021). *Laguna Water District, Laguna Annual Audit Report 2020*. https://www.coa.gov.ph/wpfd_file/laguna-water-district-laguna-annual-audit-report-2020/

[11] Commission on Audit. (2023). *Laguna Water District, Laguna Annual Audit Report 2022*. https://www.coa.gov.ph/wpfd_file/laguna-water-district-laguna-annual-audit-report-2022/

[12] Nidheesh, P., & Singh, T. A. (2017). Arsenic removal by electrocoagulation process: Recent trends and removal mechanism. *Chemosphere*, *181*, 418–432. https://doi.org/10.1016/j.chemosphere.2017.04.082

[13] Song, P., Yang, Z., Zeng, G., Yang, X., Xu, H., Wang, L., Xu, R., Xiong, W., & Ahmad, K. (2017). Electrocoagulation treatment of arsenic in wastewaters: A comprehensive review. *Chemical Engineering Journal*, *317*, 707–725. https://doi.org/10.1016/j.cej.2017.02.086

[14] Amrose, S. E., Bandaru, S. R., Delaire, C., van Genuchten, C. M., Dutta, A., DebSarkar, A., Orr, C., Roy, J., Das, A., & Gadgil, A. J. (2014). Electro-chemical arsenic remediation: Field trials in West Bengal. *Science of the Total Environment*, *488*, 539–546. https://doi.org/10.1016/j.scitotenv.2013.11.074

[15] van Genuchten, C. M., Peña, J., Amrose, S. E., & Gadgil, A. J. (2014). Structure of Fe (III) precipitates generated by the electrolytic dissolution of Fe (0) in the presence of groundwater ions. *Geochimica et Cosmochimica Acta*, *127*, 285–304. https://doi.org/10.1016/j.gca.2013.11.044

[16] Delaire, C., Amrose, S., Zhang, M., Hake, J., & Gadgil, A. (2017). How do operating conditions affect As (III) removal by iron electrocoagulation? *Water research*, *112*, 185–194. https://doi.org/10.1016/j.watres.2017.01.030

[17] Li, L., Li, J., Shao, C., Zhang, K., Yu, S., Gao, N., Deng, Y., & Yin, D. (2014). Arsenic removal in synthetic ground water using iron electrolysis. *Separation and Purification Technology*, *122*, 225–230. https://doi.org/10.1016/j.seppur.2013.11.012

[18] Wan, W., Pepping, T. J., Banerji, T., Chaudhari, S., & Giammar, D. E. (2011). Effects of water chemistry on arsenic removal from drinking water by electrocoagulation. *Water research*, *45*(1), 384–392. https://doi.org/10.1016/j.watres.2010.08.016

[19] Van Genuchten, C. M., Bandaru, S. R., Surorova, E., Amrose, S. E., Gadgil, A. J., & Pena, J. (2016). Formation of macroscopic surface layers on Fe (0) electrocoagulation electrodes during an extended field trial of arsenic treatment. *Chemosphere*, *153*, 270–279. https://doi.org/10.1016/j.chemosphere.2016.03.027

[20] Banerji, T., & Chaudhari, S. (2016). Arsenic removal from drinking water by electrocoagulation using iron electrodes-an understanding of the process parameters. *Journal of Environmental Chemical Engineering*, *4*(4), 3990–4000. https://doi.org/10.1016/j.jece.2016.09.007

[21] Amrose, S., Gadgil, A., Srinivasan, V., Kowolik, K., Muller, M., Huang, J., & Kostecki, R. (2013). Arsenic removal from groundwater using iron electrocoagulation: Effect of charge dosage rate. *Journal of Environmental Science and Health, Part A*, *48*(9), 1019–1030. https://doi.org/10.1080/10934529.2013.773215

[22] Dutta, N., Haldar, A., & Gupta, A. (2021). Electrocoagulation for arsenic removal: Field trials in rural West Bengal. *Archives of environmental contamination and toxicology*, *80*(1), 248–258. https://doi.org/10.1007/s00244-020-00799-8

[23] Kobya, M., Demirbas, E., & Ulu, F. (2016). Evaluation of operating parameters with respect to charge loading on the removal efficiency of arsenic from potable water by electrocoagulation. *Journal of environmental chemical engineering*, *4*(2), 1484–1494. https://doi.org/10.1016/j.jece.2016.02.016

[24] Balares, K. L., Nuevo, J., Chiong, M., Macasieb, R., Resurreccion, A., & Orozco, C. (2020). Estimating Energy Consumption and Cost for the Electrocoagulation of Arsenic-laden Water (ECAR) Using Iron Electrodes. *E3S Web of Conferences*, *148*, 01004. https://doi.org/10.1051/e3sconf/202014801004

[25] van Genuchten, C. M., Gadgil, A. J., & Peña, J. (2014). Fe (III) nucleation in the presence of bivalent cations and oxyanions leads to subnanoscale 7 Å polymers. *Environmental science & technology*, *48*(20), 11828–11836. https://doi.org/10.1021/es503281a

[26] Catrouillet, C., Hirosue, S., Manetti, N., Boureau, V., & Peña, J. (2020). Coupled As and Mn redox transformations in an Fe (0) electrocoagulation system: Competition for reactive oxidants and sorption sites. *Environmental science & technology*, *54*(12), 7165–7174. https://doi.org/10.1021/acs.est.9b07099

[27] Dutta, N., & Gupta, A. (2022). Development of arsenic removal unit with electrocoagulation and activated alumina sorption: Field trial at rural west bengal, india. *Journal of Water Process Engineering*, *49*, 103013. https://doi.org/10.1016/j.jwpe.2022.103013

[28] Schloerke, B. e. a. (2024). *GGally: Extension to "ggplot2"*. cran.r-project. https://cran.r-project.org/web/packages/GGally/GGally.pdf

[29] Wood, S. N. (2011). Fast stable restricted maximum likelihood and marginal likelihood estimation of semiparametric generalized linear models. *Journal of the Royal Statistical Society Series B: Statistical Methodology*, *73*(1), 3–36. https://doi.org/10.1111/j.1467-9868.2010.00749.x

[30] Liu, Y., Li, Y., Yin, W., Wang, H.-c., Zhao, X., Liu, X., Lu, S., & Wang, A.-j. (2024). Long-term performance of a deep oxidation pond with horizontal subsurface flow constructed wetland for purification of rural polluted river water. *Environmental Research*, *240*, 117498. https://doi.org/10.1016/j.envres.2023.117498

[31] Liu, X., Wang, Y., Lu, S., Liu, Y., Zhao, B., Xi, B., Guo, X., Guo, W., & Zhang, J. (2020). Intensified sulfamethoxazole removal in an electrolysis-integrated tidal flow constructed wetland system. *Chemical Engineering Journal*, *390*, 124545. https://doi.org/10.1016/j.cej.2020.124545

[32] Amin, R., Salan, M. S. A., & Hossain, M. M. (2024). Measuring the impact of responsible factors on CO2 emission using generalized additive model (GAM). *Heliyon*, *10*(4), e25416. https://doi.org/10.1016/j.heliyon.2024.e25416

[33] Ye, Z., Hong, S., He, C., Zhang, Y., Wang, Y., Zhu, H., & Hou, H. (2022). Evaluation of different factors on metal leaching from nickel tailings using generalized additive model (GAM). *Ecotoxicology and Environmental Safety*, *236*, 113488. https://doi.org/10.1016/j.ecoenv.2022.113488

[34] da Silva Marques, D., Costa, P. G., Souza, G. M., Cardozo, J. G., Barcarolli, I. F., & Bianchini, A. (2019). Selection of biochemical and physiological parameters in the croaker Micropogonias furnieri as biomarkers of chemical contamination in estuaries using a generalized additive model (GAM). *Science of the Total Environment*, *647*, 1456–1467. https://doi.org/10.1016/j.scitotenv.2018.08.049

[35] Wood, S. N. (2017). *Generalized additive models: An introduction with R (Texts in Statistical Science)*. Chapman Hall/CRC.

[36] Arel-Bundock, V., Greifer, N., & Heiss, A. (2024). How to interpret statistical models using marginal effects in R and Python. *Journal of Statistical Software*, *55*(2), 1–31. https://marginaleffects.com/assets/marginaleffects_arel-bundock_greifer_heiss_jss5115.pdf

[37] Dubrawski, K. L., van Genuchten, C. M., Delaire, C., Amrose, S. E., Gadgil, A. J., & Mohseni, M. (2015). Production and transformation of mixed-valent nanoparticles generated by Fe (0) electrocoagulation. *Environmental science & technology*, *49*(4), 2171–2179. https://doi.org/10.1021/es505059d

[38] Mosivand, S., & Kazeminezhad, I. (2015). A novel synthesis method for manganese ferrite nanopowders: The effect of manganese salt as inorganic additive in electrosynthesis cell. *Ceramics International*, *41*(7), 8637–8642. https://doi.org/10.1016/j.ceramint.2015.03.074

[39] Dancey, C., & Reidy, J. (2020). *Statistics without maths for psychology*. Pearson Education.